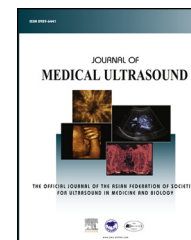


Available online at [www.sciencedirect.com](http://www.sciencedirect.com)

ScienceDirect

journal homepage: [www.jmu-online.com](http://www.jmu-online.com)

## REVIEW ARTICLE

# Microbubble-enhanced Focused Ultrasound-induced Blood–brain Barrier Opening for Local and Transient Drug Delivery in Central Nervous System Disease



Ching-Hsiang Fan, Chih-Kuang Yeh\*

Department of Biomedical Engineering and Environmental Sciences, National Tsing Hua University, Hsinchu, Taiwan

Received 4 October 2014; accepted 11 November 2014  
Available online 17 December 2014

**KEY WORDS**

blood–brain barrier,  
central nervous  
system disease,  
focused ultrasound,  
microbubbles

The blood–brain barrier is a specialized protective structure in the central nervous system, which is critical for maintaining brain homeostasis and low permeability to control the passage of molecules from the circulation into the brain parenchyma and the efflux from the brain. However, the blood–brain barrier also hinders the transportation of therapeutic agents and contrast agents from the blood into brain tissue, lowering treatment efficiency. Recently, focused ultrasound sonication with microbubbles has been proved to transiently open the blood–brain barrier, allowing the penetration of administered agents or drugs into the brain. In this article, we review the current state of this drug delivery technique, its application in preclinical brain disease models, and treatment planning for this novel technique.

© 2014, Elsevier Taiwan LLC and the Chinese Taipei Society of Ultrasound in Medicine. All rights reserved.

## Blood–brain barrier

### Concept of the blood–brain barrier

The blood–brain barrier (BBB) was first discovered by Paul Ehrlich [1]. He noted that when he administered a dye into an *in vivo* circulatory system, all the organs were stained except for the brain and the spinal cord. Further evidence of the BBB was provided by Max Lewandowsky [2] and Edwin Goldmann [3]. Lewandowsky [2] discovered the limited

Conflicts of interest: The authors declare no conflicts of interest.

\* Correspondence to: Professor Chih-Kuang Yeh, Department of Biomedical Engineering and Environmental Sciences, National Tsing Hua University, Number 101, Section 2, Kuang-Fu Road, Hsinchu 30013, Taiwan.

E-mail address: [ckye@mx.nthu.edu.tw](mailto:ckye@mx.nthu.edu.tw) (C.-K. Yeh).

<http://dx.doi.org/10.1016/j.jmu.2014.11.001>

0929-6441/© 2014, Elsevier Taiwan LLC and the Chinese Taipei Society of Ultrasound in Medicine. All rights reserved.

permeability of potassium ferrocyanate into the brain, and Goldmann [3] noticed that when he directly injected trypan blue dye into the cerebrospinal fluid, only cells within the brain were stained. Although these findings offered indications for the presence of the BBB, the concept of the BBB was confirmed by Davson and Spaziani [4], who demonstrated that cerebral capillaries prevent the diffusion of sucrose, iodide, and p-aminohippurate into the brain. In 1967, Reese and Karnovsky [5] designed further experiments to visualize the BBB using horseradish peroxidase.

### Structure of the BBB

The capillary network within the brain is extremely packed (about 20 m<sup>2</sup>/1300 g in human brain [6]) and is intricate. Thus, each neuron is perfused by its own microvasculature [7]. The BBB is a specialized substructure within the central nervous system (CNS) blood vascular system, which consists of endothelial cells (ECs) connected together by tight junctions (TJs), basement membranes, pericytes, and astrocytes [8]. This layered structure acts as the brain's frontline defense against toxic and harmful materials in the blood stream. The TJs are located in the cerebrovascular endothelium, which contains membrane-associated guanylate kinases such as cingulin, occludin, and the cadherins (single-pass membrane-spanning molecules) ZO-1 and ZO-2 [9]. The presence of TJs prevents circulating substances from entering the brain via paracellular routes, although they can reach the brain through the ECs of brain microvessels via a transcellular pathway or via specialized receptor-mediated transcytosis and transport proteins [10]. The basement membrane supports the abluminal surface of the astrocytes, ECs, and pericytes [11]. The combination of ECs, astrocyte feet, and pericytes makes the BBB less permeable to large-molecular-weight (>500 Da) [12], water-soluble, and ionic substances [13]. Therefore, the BBB prevents nearly 100% of macromolecule therapeutic drugs and diagnostic substances, and about 98% of small-molecule agents from penetrating the brain, which is a great disadvantage for the treatment of CNS disease [14].

### Methods for increasing BBB permeability

There are a number of preclinical and clinical approaches for crossing the BBB to enhance drug delivery into the brain tissue, including: (1) chemical modification of drugs to make them lipophilic, (2) use of drug carriers to transport drugs across the BBB, (3) intravenous (i.v.) administration of hypertonic solutions to open the BBB, and (4) direct transcranial injection of drugs through a needle or catheter to bypass the BBB structure and reach the brain. In approach (1), the drug is modified with lipid-soluble functional groups (e.g., amino acids) or conjugated to lipid carriers (e.g., free fatty acid, adamantane, or dihydropyridine) to achieve drug lipidization. However, the main problem with drug lipidization lies in the increased uptake of the lipidized drug by peripheral organs, reducing the drug concentration in the brain tumor [7]. In approach (2), the drug is encapsulated into carriers (e.g., liposomes or nanoparticles [15]), or conjugated to proteins [16], peptide

vectors [17], or antibodies [18]. These drug carrier devices then promote the transportation of the drug across the BBB using a BBB endogenous-carrier system and/or a receptor-mediated transcytosis route. Due to the finite amount of receptors *in vivo* and the limited payload of a drug carrier, the drug carrier approach is limited by inadequate transportation of the drug. In approach (3), the infusion of hyperosmotic solution (e.g., mannitol and arabinose) induces shrinkage of the brain and brain capillary ECs, and thus leads to a transient opening of the TJs [19]. However, this method induces nonlocalized drug delivery as well as promotes the penetration of toxic substance into the brain tissues (e.g., plasma albumin or other blood protein components), thereby causing damage to surrounding normal brain cells and neural cells [20]. In approach (4), the drug is directly delivered to the brain via either an intracerebroventricular injection or an intracerebral implantation [21]. Nevertheless, the drug can only penetrate the brain tissue via diffusion, which makes it difficult to cover the whole lesion from the depot site. Further, this method may produce invasive traumas during the injection process.

### Therapeutic effect of focused ultrasound

The piezoelectric materials of an ultrasound probe can be manufactured into an arc shape, or electric phase modulation can be used to focus transmitted ultrasound energy, thus enabling focused ultrasound (FUS). FUS allows noninvasive accumulation of acoustic energy within a focal spot inside the body, with negligible biological effects to the surrounding tissues and near-fields. There are two kinds of mechanisms for inducing biological effects by FUS, thermal and nonthermal (e.g., cavitation), both of which are discussed below.

When exposing biological tissues to FUS for long durations, the acoustic energy is attenuated and absorbed by the surrounding tissues, and then converted into thermal energy, producing a regional temperature rise. This temperature-rising phenomenon has been shown to persist for minutes to hours, and is further introduced in treatment applications, called hyperthermia. However, previous studies have indicated that temperatures in the range of 43–46°C have detrimental effects on the brain tissue such as ammonia production, hemiparesis, and even death [22]. By contrast, tumor cells are believed to be particularly sensitive to heat, and therefore, FUS-induced hyperthermia (at 43°C for 30–60 minutes) can be used to increase the sensitivity of tumors to other interventions (radiation therapy, chemotherapy, and immunotherapy) used to treat cancers [23]. At higher temperatures (>60°C), FUS is also applied as a thermal ablation procedure to defeat solid tumors. Many studies have demonstrated the feasibility of using thermal ablation to remedy a variety of tumors, including kidney, uterus, liver, breast, bone, pancreas, and prostate [24,25]. In addition, thermal coagulation of blood vessels has also been proposed as a medical application of FUS [26,27].

One major limitation of ultrasound-induced thermal therapy in the brain is the strong absorption and attenuation of acoustic energy by the skull. Therefore, for clinical brain therapeutic application, an invasive craniotomy is

essential. Recently, transcranial FUS sonication of the brain parenchyma has been proposed by using a phased array system to minimize the attenuation and distortion of ultrasound waves caused by the skull [28,29]. The optimal frequency of transcranial sonication is confirmed to be <1 MHz [29]; however, due to its larger focal spot and reduced pressure gain, low-frequency ultrasound does not allow energy focusing as sharply as high frequency does, thus making it possible to overheat the skull [30].

Many studies have reported that acoustic-driven cavitation can be used to enhance tissue heating during FUS sonication [31]. Unlike rigid particles, the highly compressible shell of microbubbles (MBs) enables oscillation (i.e., MBs can expand and contract in size) in response to the pressure changes of a FUS pulse. There are two modes of cavitation when the MBs are placed in an ultrasound field: stable and inertial cavitation. Stable cavitation causes MBs to oscillate coherently with the incident ultrasound pulse, resulting in the generation of not only nonlinear harmonic ultrasound waves of the transmitted fundamental frequency [i.e., half the fundamental frequency (subharmonics), 2-fold of the fundamental frequency (2<sup>nd</sup> harmonics), etc.] [32], but also strong liquid flows around the MBs (e.g., microstream) [33]. At higher acoustic pressures, the MBs grow rapidly during the rarefaction phase of ultrasound and violently collapse due to the inertia of the intruding fluid. This type of cavitation is referred to as inertial cavitation. The collapse of MBs splits them into many smaller MBs and even fragmentations, producing wideband signals that are usually recognized as a signature of inertial cavitation. During the inertial cavitation, shock waves and transient high temperature (reportedly up to 5000 K) are generated in the fluid nearby the MBs. In addition, the liquid jet formation is located close to the cell membrane, increasing the permeability of the cell [34]. Furthermore, many groups have demonstrated the *in vivo* applications of combining MBs and FUS to achieve local, temporary, and reversible BBB opening [35].

## Interaction between FUS and MBs within brain tissue

### Combining MBs and FUS-induced BBB opening for CNS drug delivery

Over a decade ago, Hynynen et al [36] proposed an innovative method utilizing FUS in combination with gas-filled MBs that were injected into the blood stream prior to FUS sonication, to noninvasively, restorably, and locally induce BBB opening. Although FUS itself has been approved to open the BBB, the addition of MBs reduces the ultrasound energy required for BBB opening, decreasing the probability of occurrence of thermal damage to the brain. This phenomenon has been supported by several reports demonstrating that the FUS-sonicated MBs are restrained in the blood vessels; hence, the elicited biological effects should be confined to the vessel walls [37,38]. Compared to other traditional brain drug delivery approaches such as hypertonic infusion of modified lipophilic chemicals, the combination of MBs with FUS is a totally noninvasive and local procedure, thus minimizing undesired off-target effects.

Further, this recoverable MB-enhanced FUS-induced BBB opening (MB-FUS-BBB opening) technique provides a time window of several hours that not only is beneficial to the transportation of drugs into the CNS, but also allows enhanced permeability and retention of drugs, specifically in the tumor. This technique provides an attractive choice for increasing the local concentration of chemotherapeutic drug for the treatment of CNS disease and brain tumors.

The feasibility of applying MB-FUS-BBB opening technique in large animals has been widely investigated by various groups. Xie et al [38] first applied this technique in the pig model, and confirmed that either albumin-coated perfluorocarbon MBs or lipid-encapsulated perfluorocarbon MBs combined with transtemporal unfocused 1-MHz FUS sonication successfully increased BBB permeability transiently. Another study conducted by Liu et al [39] showed that BBB opening can be transtemporally achieved in swine using very-low-frequency ultrasound (28 kHz) with a planar transducer. After performing craniotomy, the distribution and penetration depth of delivered superparamagnetic iron oxide (SPIO) within brain tissue were further enhanced. However, the low-frequency ultrasound resulted in off-target effects, since ultrasound waves reflect within the skull cavity.

Nonhuman primate MB-FUS-BBB opening has also been studied. McDannold et al [40] showed that repeated and recoverable BBB opening was achieved in rhesus macaques. In addition, none of the animals that underwent the BBB opening process had evident histological or functional damage. Another initial study by Marquet et al [41] demonstrated the feasibility of combining two different types of MBs (customized 4–5  $\mu\text{m}$  and Definity) with 500 kHz FUS in primates. It is noteworthy that in the primate model, monitoring of the transcranial cavitation during BBB opening can still be achieved by a passive cavitation detector. Tung et al [42] also reported the feasibility of transcranial, cavitation-guided BBB opening in a monkey. However, the number of cases and data for successful BBB openings are limited. Moreover, prior studies lack histological confirmation or cognitive test results.

## Cellular mechanisms of MB–FUS–BBB opening

There are four possible routes by which macromolecules can cross the BBB after FUS is performed with MBs: (1) transcytosis; (2) transendothelial cell cytoplasmic openings; (3) interendothelial clefts via opening of a part of the TJs; and (4) free passage through the damaged EC lining [43]. After BBB opening, active vesicular transport occurs first [44]. Several electron microscopy studies have reported that the vesicle number within the ECs of the BBB [43–45] and blood–tumor barrier (BTB) [46] increases following FUS sonication. Furthermore, the interactions of FUS and MBs transiently upregulate the caveolae proteins within the BTB and the BBB [45,46].

The other mechanism for transfer of macromolecules into the brain parenchyma is paracellular passage through the interendothelial clefts and opened TJs. The former has been visualized by electron microscopy [47], and proteins of TJ (e.g., claudin-1, claudin-5, ZO-1, and occludin) are downregulated in the FUS-induced BBB opening region

[48,49]. Moreover, FUS sonication promotes phosphorylation of AKT (also known as protein kinase B), which may change the integrity of TJs [49]. Both *in vitro* and *in vivo* studies demonstrated that ion imbalances (e.g.,  $\text{Ca}^{2+}$ ) induced by FUS are associated with cellular sonoporation reorganization of gap junction proteins [50].

By contrast, *in vivo* microvasculature dynamic imaging during BBB opening has been conducted by multiphoton microscopy [51]. Both vasoconstriction and vasodilation have been reported after applying MBs and FUS; however, vasoconstriction seems to appear only in arterioles [52]. In addition, leakage of the agent (i.e., dyes) after MB-FUS-BBB opening can be divided into three categories: (1) fast; (2) sustained; and (3) slow [53]. Choe et al showed that fast leakage brought about a rapid enhancement in dye signal intensity within the extravasculature, reaching a peak within 1 minute after MB-FUS-BBB opening, followed by a quick decrease. This type of leakage occurred in case of all vessels sizes and acoustic pressures (0.071–0.25 MPa) in their study. In addition, this leakage occurred at the vessel wall with point sources. The leakage response of sustained leakage resembled fast leakage, but the dye signal intensity kept increasing after FUS sonication, which lasted for 1 hour. Sustained leakage occurred at low-to-intermediate pressures (0.071–0.13 MPa), and compared to fast leakage, sustained leakage involved vessels of similar diameters, but within a smaller range of sizes. Ultimately, slow leakage happened 5–15 minutes after applying FUS irradiation with low acoustic pressures (0.071–0.1 MPa) and was more prevalent among small vessels (<25  $\mu\text{m}$ ).

## Bioeffects of FUS and MBs

Notwithstanding the abovementioned benefits of MB-FUS-BBB opening, there is still a concern that the inertial cavitation that occurs during the BBB opening process may generate high-velocity jets, shock waves, and free radicals that should damage the ambient cellular structures, producing undesired complications within the sonicated location, including intracerebral hemorrhage (ICH), transient blood-supply shortage, cellular inflammation response, and cell apoptosis [53,54]. Many studies have indicated that the occurrence of ICH is associated with most of the immediate and delayed brain injuries [55]. Furthermore, the ICH limits the permeability of the BBB, decreasing the efficiency of drug delivery into the brain [56].

There are several reasons why ICH induces brain injuries: (1) chemical toxicity from the hematoma or the mechanical forces that appear during hematoma formation may cause cellular apoptosis and necrosis adjacent to the ICH regions [57]; (2) formation of edema following ICH increases intracranial pressure and produces herniation [58]; (3) the cerebral metabolic rate of oxygen and cerebral blood flow decrease around the ICH zone [59]; (4) thrombin production immediately after ICH may cause inflammatory cell infiltration and brain edema [60]; (5) erythrocyte lysis occurs during the formation of the membrane attack complex after activation of the complement cascade and depletion of intracellular energy [61]; (6) overloading of iron in the ICH area causes local epileptiform paroxysmal discharges [62]; and (7) the interaction between thrombin

and iron may damage the brain after ICH because thrombin upregulates the transferrin receptor of the brain, causing excessive iron uptake into the cells [63].

## MB-FUS-BBB opening for enhanced delivery of agents into the brain

There have been a number of efforts to deliver molecules across an intact BBB by MB-FUS-BBB opening with preclinical setups. Trypan blue (872.8 Da) and Evans blue (960.8 Da) dyes are extensively utilized to confirm successful BBB opening [64,65]. In addition, gadolinium-based contrast agents (Gd, 500–900 Da) used for magnetic resonance imaging (MRI) are frequently administered to confirm the site and efficiency of the BBB opening [66,67]. Other imaging tracers such as horseradish peroxidase (40 kDa) [68,69], Alexa Fluoro 488 (10 kDa) [50], monocrySTALLINE iron oxide nanoparticles (10 kDa) [51], Texas red-tagged dextran (3–70 kDa) [52,70], lanthanum chloride (139 Da) [69],  $^{99\text{m}}\text{Tc}$  diethylenetriaminepentaacetate (492 Da) [70], SPIO (60 nm) [71],  $\text{Mn}^{2+}$  [72], and gold nanorods [73] all have been delivered across the BBB.

In terms of therapeutic molecules and antitumor drugs (Table 1), Kinoshita et al [74] successfully delivered Herceptin (150 kDa) and D4 receptor antibodies (150 kDa) into mouse brain tissues [65]. Treat et al [75] demonstrated successful delivery of doxorubicin (DOX) (543 Da) into normal rat brain through MB-FUS-BBB opening. Wu et al [76] reported that the level of methotrexate (545.44 Da) that accumulated into the brain by MB-FUS-BBB opening was higher than that by intracarotid injection. Several studies have also shown that deposition of liposomal DOX, 1,3-bis(2-chloroethyl)-1-nitrosourea (BCNU), temozolomide, and boronophenylalanine can also be enhanced by MB-FUS-BBB opening in a rat glioma model [56,77–80].

In addition, many studies have focused on the delivery of other therapeutic substances (e.g., DNA, antibody, macrophage, or stem cells) into the brain. The anti-amyloid- $\beta$  antibodies (150 kDa) and BAM-10 antibodies can also cross the BBB in a mouse model of Alzheimer's disease (AD) [81,82]. Recently, neural stem cells have been transported into brain by an MB-FUS-BBB opening technique [83]. Burgess et al [84,85] showed that the siRNA can be noninvasively delivered into the striatum by MB-FUS-BBB opening in a mouse model of Huntington's disease (HD). The feasibility of transferring brain-derived neurotrophic factor by DNA-loaded MBs and FUS for gene therapy in the brain has been conducted by Huang et al [86]. In virus-based gene delivery, Hsu et al [87] showed that following MB-FUS-BBB opening, the recombinant adeno-associated viral vectors can be noninvasively and locally delivered into brain tissues, achieving the goal of targeted gene delivery.

## Treatment efficiency of MB-FUS-BBB opening on brain disease models

### Brain tumor

Despite the enhanced delivery of agents by MB-FUS-BBB opening, it is also important to demonstrate the

**Table 1** Summary of therapeutic agents that have been delivered across the BBB or BTB by MB-FUS-BBB opening.

Therapeutic agent	Use	Animal model
Herceptin	Anticancer antibody	Normal brain [74] Breast cancer brain model [93]
D4 receptor antibodies	Treating CNS disease	Normal brain [65]
DOX	Treating brain tumor	Normal brain [75]
Methotrexate	Treating brain tumor	Normal brain [76]
Liposomal DOX	Treating brain tumor	Gliosarcoma model [77]
BCNU	Treating brain tumor	Glioblastoma model [56]
Temozolomide	Treating brain tumor	Glioblastoma model [78]
Boronophenylalanine	Treating brain tumor	Gliosarcoma model [80]
Anti-A $\beta$ antibodies	Treating AD	AD model [81]
Anti-A $\beta$ antibodies	Treating AD	AD model [82]
Stem cells	Gene therapy	Normal brain [83]
siRNA	Treating HD	HD model [84]
siRNA	Treating HD	HD model [85]
pBDNF-EGFP-N1	Gene therapy	Normal brain [86]
Adeno-associated virus	Gene therapy	Normal brain [87]
Epirubicin in magnetic nanoparticles	Treating brain tumor	Gliosarcoma model [95]
BCNU-VEGF <sup>a</sup>	Treating brain tumor	Glioblastoma model [128]
DOX-SPIO <sup>a</sup>	Treating brain tumor	Glioblastoma model [94]
BCNU <sup>a</sup>	Treating brain tumor	Glioblastoma model [129]
BCNU <sup>a</sup>	Treating brain tumor	Normal brain [123]
GDNF <sup>a</sup>	Treating brain injury	Neonatal rat brain [99]
GDNF <sup>a</sup>	Treating PD	PD model [100]

AD = Alzheimer's disease; BBB = blood-brain barrier; BTB = blood-tumor barrier; CNS = central nervous system; FUS = focused ultrasound; GDNF = glial cell-derived neurotrophic factor; HD = Huntington's disease; MB = microbubble; PD = Parkinson's disease; SPIO = superparamagnetic iron oxide; VEGF = vascular endothelial growth factor; DOX = doxorubicin; BCNU = 1,3-bis(2-chloroethyl)-1-nitrosourea.

<sup>a</sup> Drug-loaded microbubbles were used.

therapeutic or diagnostic response in a CNS disease model. Brain tumors (including glioma, glioblastoma multiforme, medulloblastoma, and astrocytoma) exhibit high lethality, but the incidence is low compared to that of other cancers. In the United States, nearly 18,000 patients are identified with malignant brain tumor, and more than half of them have Glioblastoma multiforme (GBM) [88]. Generally, the patients with low-grade gliomas have a median survival of

5–15 years. However, because of the poor prognosis of high-grade gliomas (e.g., GBM), the median survival of the patients is only 9–12 months [89]. In addition, most brain tumors may recur locally within the site of the original lesion [78].

Chemotherapy is a widespread treatment choice for brain tumor. However, the major obstacle to brain tumor chemotherapy is the BTB, which is the BBB surrounding the tumor with a few different characteristics from the BBB [90]. Permeability of the BTB within the brain tumor is highly heterogeneous and is associated with tumor regions, resulting in the extraordinarily variable BTB integrity within different areas of the same tumor [91,92]. Generally, the leakiest region of the BTB in a malignant brain tumor is often present in the core of the tumor, while the BTB structure at the peripheral edge of the proliferating tumor is relatively intact [93]. The appearance of the BTB around the brain tumor not only hampers the treatment outcome on BBB intact tumor-infiltrating regions (typically in the tumor periphery), but also serves as a critical reason for high GBM recurrence. Thus, one of the essential issues for brain tumor therapy is to further increase the BBB integrity of the tumor periphery. Liu et al [56] and Fan et al [94] indicated that the permeability of BTB can be further increased by FUS and MBs. Several studies have shown that the combination of FUS and MBs can enhance the penetration of drugs across the BTB to control tumor progression and prolong animal survival, in an orthotopic rodent model of glioblastoma multiforme [56,77,78]. Park et al [93] further demonstrated that the growth inhibition of metastatic brain tumors can be improved by this technique. Liu et al [56] showed that with MB-FUS-BBB opening, the amount of free BCNU accumulated within rat C6 glioma tumor was enhanced. They also showed that magnetic nanoparticles (6–12 nm) conjugated with epirubicin (543.5 Da) can be successfully delivered to rat C6 glioma tumor, causing a reduction in tumor size [95]. Recently, their group demonstrated that the local concentration of temozolomide can be increased by performing MB-FUS-BBB opening, thus improving the control of tumor progression and animal survival [81]. Other recent studies have presented enhanced delivery of boronophenylalanine by MB-FUS-BBB opening, increasing the treatment efficiency of boron neutron capture therapy for the rat GBM model and 9L gliosarcoma tumor rat model [82,83].

While these studies have shown positive results in terms of an antitumor effect, there are still many issues that need to be investigated. The first factor is that the penetration area of the drugs should include infiltrating tumor cells. Novel orthotopic models only provide limited tumor infiltrating zones, so it is essential to evaluate the therapeutic efficiency of tumor regions that are outside of the FUS sonication area. The second factor is related to the parameters of FUS. Liu et al [56] have demonstrated that overexcitation of FUS can induce the occurrence of ICH, which leads to BCNU hydrolysis, thereby decreasing the amount of drug entering the brain. However, MB-FUS-BBB opening induced cellular inflammation, which has been reported to have an antitumor effect [96]. Therefore, optimization of FUS parameters should be the next issue for improving tumor treatment outcome. This technique can open the BBB transiently and the blood lifetime of the drug

is limited, so selecting a time point that can maximize the amount of drug entering the whole tumor cell is the third issue. Although many questions remain to be answered, the advancement of this technology will contribute significantly to brain neuro-oncology treatments.

### Parkinson's disease

In addition to applications in the treatment of brain tumors, the feasibility and treatment effect of MB-FUS-BBB opening should be discussed for CNS neurodegenerative diseases. Parkinson's disease (PD) is a neurodegenerative disease associated with depleted dopamine production, which causes tremor, muscular rigidity, bradykinesia, gait difficulty, akinesia, and even death of part of the brain in the most serious cases [97]. The available symptomatic treatments for PD currently include medical and surgical modalities and gene therapy, of which surgery is an extremely invasive and highly complex approach. Medication primarily focuses on dopamine supplementation to relieve the motor symptoms [98]. The clinical effectiveness of dopamine, however, is limited by the BBB, which prevents the drugs from entering the brain parenchyma. Moreover, as the neuron degeneration progresses, the medical management of PD becomes more complex and medications become less effective. Therefore, development of an endogenous dopamine generative mechanism is an urgent consideration for PD, and gene-based techniques have recently been proposed to replace missing or dysfunctional genes in order to synthesize dopamine. Glial cell-derived neurotrophic factor (GDNF) has been shown to provide a neuroprotective effect in PD rats. Wang et al [99] first proposed lipid-coated GDNF-loaded MBs. With sonication of FUS, these MBs can release GDNF to ameliorate hypoxia–ischemia injury in neonatal rats. In 2014, they investigated the neuroprotective effect by further applying this treatment method to a PD rat model. Their results showed that this treatment method reduced apomorphine-induced rotations, and increased striatal dopamine and nigral tyrosine hydroxylase levels in PD rats 4 weeks after performing the treatment [100]. While levodopa remains the most effective drug in the treatment of PD, long-term levodopa administration causes dyskinesia, which has hindered its use in PD patients. The ultrasound-induced lipid-coated GDNF MBs constitute another effective drug therapy for the treatment of PD.

### Alzheimer's disease

AD is characterized as a neurodegenerative and progressive disease without available treatment in aged humans. The clinical symptoms of AD include gradual decline in cognitive function, memory loss, trouble with language, and mood swings [101,102]. The pathogenesis of AD is believed to be driven by the production and accumulation of the hyperphosphorylated tau and beta-amyloid (A $\beta$ ), which aggregate and form tau tangles, amyloid, and plaques [103]. Current therapeutic and diagnostic management is focused on reducing and discovering A $\beta$  aggregates [104,105]. The common treatment of AD patients is the long-term i.v. injection of high doses of anti-A $\beta$  antibody to clear A $\beta$

plaques in the brain [106]. However, only 0.1% of injected antibodies arrive in the lesion in this way [107]. Other delivery methods include direct delivery of anti-A $\beta$  antibody into the cortex by intracranial injection or skull removal [105,108]. Although the plaques can be reduced within a few days, the drawback of these procedures is its invasive nature. Raymond et al [82] first demonstrated that MB-FUS-BBB opening allows the delivery of both small antibodies and molecules in the AD mouse model (B6C3-tg). The treatment efficiency of MB-FUS-BBB opening with immunotherapy for a different AD mouse model (TgCRND8) was evaluated by Jordão et al [81]. They showed that A $\beta$  plaques were significantly reduced 4 days after treatment with a lower dose of antibody than used in previous studies. Recently, Jordão et al [109] observed that A $\beta$  plaque size and number were significantly reduced within 4 days following the process of MB-FUS-BBB opening in TgCRND8 mice. In 2014, Burgess et al [110] validated that repeated MB-FUS-BBB opening targeted to the hippocampus could modulate pathologic abnormalities, plasticity, and behavior in the same animal model. There are two potential mechanisms for FUS-enhanced A $\beta$  internalization and clearance. First, opening of the BBB permits the entry of endogenous immunoglobulin G and immunoglobulin M from the periphery into the brain. Second, FUS causes activation of astrocytes and microglia. By contrast, properties of cerebral vessels in AD mouse and healthy mouse were investigated by two-photon microscopy and fluorescent dextran [111]. Burgess et al [111] noticed that the change in cerebral vascular diameter might depend on BBB permeability, and the occurrence of A $\beta$  plaques might reduce the permeability of a vessel after FUS sonication because the plaques deposited on the vessel wall weaken the vessel structure and reduce the elastic properties. Their results revealed the impact of vascular amyloid on the MB-FUS-BBB opening, thus increasing the safety of this technique for AD patients in the future.

### Huntington's disease

HD is a dominantly inherited neurodegenerative disorder. The mechanism of HD is an unstable expansion of a CAG triplet repeat stretch within the Huntingtin (*Htt*) gene [112]. This mutation results in a variant HTT protein that gradually produces cell death and neuronal dysfunction in the brain. Symptoms of HD are motor dysfunction, cognitive decline, and progressive emotional changes. While HD is monogenic and the etiology is known, there is still no available treatment. Tetrabenazine is approved for reducing the severity of its symptoms, but the side effects include akathisia, depression, and dizziness [113,114]. In addition, drug efficiency decreases as HD progresses. Recently, because RNA interference can specifically reduce the expression of the mutant *Htt*, gene therapy has been proposed for the treatment of HD [115]. However, due to its high molecular weight, the RNA does not pass through the BBB, and thus delivery into the brain is limited to direct CNS delivery. Burgess et al [85] have shown, in a rat HD model, that the MB-FUS-BBB opening is an effective strategy for noninvasively delivering cholesterol-conjugated small interfering RNA to the striatum. In addition, their data

illustrated that a significant reduction of *Htt* expression can be observed 48 hours after treatment and this reduction in *Htt* expression is higher when the extent of BBB opening is increased. This study was a good beginning for demonstrating that RNA treatment for knockdown of mutant *Htt* is feasible without surgical delivery to the brain.

## Techniques to plan, monitor, and estimate MB-FUS-BBB opening

### Treatment plan and consideration

The first condition that should be considered prior to using MB-FUS-BBB opening in an animal model is the accuracy. In general, accurate FUS sonication can be conducted with stereotactic frames [67]. Relying on trustworthy and repeatable data, FUS can be delivered into a targeted brain location without imaging guidance through a craniotomy. Hynynen et al [36] first demonstrated a MRI-guidance FUS system for precisely targeting and monitoring of transcranial MB-FUS-BBB opening by MRI guidance. The second concern is the occurrence of standing waves during transcranial sonication. Standing waves can be eliminated by a wideband composite sharply focused transducer and a reduced duty cycle to disrupt the BBB without brain damage [116].

The major obstacle of applying this approach to human is the skull. Due to the thickness and irregular shape of the skull, the FUS beam passing through different parts of the skull can be deflected and distorted [117]. In addition, the high attenuation of FUS would lead to a rise in the temperature of the skull. The hemispherical phased array proposed by Clement et al [118] can solve these problems. First, the driving frequency of this array was 665 kHz, thus lowering energy absorption by the skull bone. Second, this array consisted of 64 elements that can be driven individually to correct for beam aberrations. Third, the temperature of the outer skull surface and scalp would be controlled within a safe range using an active cooling system.

The BBB opening effect was conducted by FUS and circulating MBs within vessels. Therefore, the intensity and the bioeffect rely on the vascularity of the targeted tissue [43]. It is essential to identify the location of FUS sonication for avoiding critical regions and large vessels. In addition, it is also important to know the perfusion ability and vascular morphology of the sonication area for optimizing FUS treatment.

### Treatment monitoring and control

After successful delivery of agents by the process of MB-FUS-BBB opening in an animal model, developing the methods for imaging this procedure will be the next important issue for applying this technique clinically. In addition, the imaging methods should not only provide the information of BBB opening, but also indicate the appearance of brain damage for increasing the safety of this technique. The first imaging modality to achieve this goal was MRI. Several studies have demonstrated that contrast-enhanced T1-weighted MRI with i.v. administration of

gadopentetate dimeglumine can be used to detect and evaluate BBB opening [39,110]. Kinetics of the BBB permeability can be measured by dynamic contrast-enhanced MRI [119]. The occurrence of ICH or inflammation caused by FUS can be visualized by T2\*- or susceptibility-weighted MRI with superparamagnetic iron oxide nanoparticles [38,74,120]. However, performing multiple MRI sequence acquisitions and acquiring high-quality images may cost on the order of minutes, restricting the use of MRI for dynamically observing the physiologic changes of BBB disruption with a temporal resolution of <1 second.

Ultrasound imaging has many properties such as high spatial resolution, and real-time and convenient imaging for various types of diagnoses. In combination with MBs, the sensitivity of ultrasound imaging can be enhanced suitably to detect the dynamic change of microcirculation and microperfusion within the brain. Goertz et al [121] first attempted to monitor the MB-FUS-BBB opening by determining the changes in the time–intensity curve of concurrent clinical ultrasound imaging. Fan et al [122] used MB destruction–replenishment time–intensity curve analysis to estimate the perfusion kinetic map for determining the scale and distribution of MB-FUS-BBB opening with a commercial ultrasound imaging system (Vevo2100; VisualSonics, Toronto, Ontario, Canada). Their results indicated that the perfusion kinetic map could provide high detection sensitivity and precision, and was highly correlated with monitoring via MRI. In addition, the occurrence of ICH also can be detected by this ultrasound imaging strategy. Although there are many limitations to the study (such as craniotomy essential and time of MB administration), this approach still provides a new opportunity to pursue ultrasound-monitored MB-FUS-BBB opening and can be a potentially valuable alternative for estimating the distribution of drug delivery.

The cavitation effect of MBs has been recognized as the major mechanism underlying the MB-FUS-BBB opening. To distinguish between the frequency components of the acquired acoustic cavitation signals emitted by oscillating MBs during the BBB opening process, the occurrence of BBB opening and brain damage should be predicted and classified in real time. McDannold et al [53] first demonstrated that the inertial cavitation is not responsible for the MB-FUS-BBB opening, and the second and third harmonics of the ultrasound driving frequency may indicate when BBB opening takes place. Tung et al [42,54] further showed that the cavitation activity during MB-FUS-BBB opening could be acquired in nonhuman primates and rodents, and inertial cavitation is not essential for BBB opening. Fan et al [123] classified the roles of stable and inertial cavitation activities during the MB-FUS-BBB opening process by matching the frequency of FUS sonication with that of self-made submicron bubbles. They verified that stable cavitation induces BBB opening, and inertial cavitation results in brain damage. They also proposed that inertial cavitation can be reduced by matching the frequency of FUS and the resonant frequency of MBs, ensuring the safety of BBB opening. O'Reilly and Hynynen [124] constructed a control algorithm to automatically adjust the acoustic pressure of FUS after each ultrasound pulse, based on acoustic emission signals captured during each burst and processed prior to the next pulse. The system can create safe BBB opening with little or

no petechiae. The potential of cavitation-guided BBB opening had been widely explored in these studies, and the feasibility of clinical applications should be investigated in the future.

### Treatment evaluation

Despite that fact that many imaging modalities can provide the information underlying MB-FUS-BBB opening, the distribution and concentration of delivered drug within the brain is still difficult to estimate. Several studies have shown the correlation between signal intensity of contrast-enhanced T1 weighted MRI and the drug concentration of brain after sonication [77,78,125]. Drug deliveries were also found to be related to the vascular transfer coefficients, via analysis of dynamic contrast-enhanced MRI [126,127]. By contrast, uptake of drugs and their penetration into the brain can be tracked if the drugs are directly labeled with a contrast agent for MRI or other imaging modality. Liu et al [95] showed the therapeutic magnetic nanoparticles not only enhance deposition in the brain, but also allow monitoring by MRI, enabling quantification of their distribution *in vivo*. Fan et al [94] fabricated SPIO-conjugated, doxorubicin-loaded MBs. After performing FUS sonication, the multifunctional MBs can concurrently open the BBB, release DOX, and act as dual ultrasound and MRI contrast agents. Due to the SPIO, nanoparticles can be monitored by MRI, and the distribution of drug can be detected and quantified during or after FUS-induced drug delivery. If the relationship between the concentration of the drug and the imaging contrast agents is revealed, we can predict the delivered drug level and therapeutic response in animal brain.

### Conclusion

The first proof-of-concept study for demonstrating the capability of MB-FUS-BBB opening in animal models was conducted in 2001. So far, the efficiency of drug delivery and the mechanism of MB-FUS-BBB opening have been extensively investigated in normal and CNS disease animal models. This technique can be used to perform noninvasive and transient drug delivery at targeted areas without the occurrence of brain damage. Many imaging modalities and methods have been developed for planning, detecting, and estimating drug delivery after performing MB-FUS-BBB opening. In addition, there have been many preclinical studies investigating its safety issues in large animals, application of FUS to human skulls, and stability of the FUS sonication device. Taken together, results from prior studies demonstrate that this drug delivery procedure is ready for clinical tests.

### References

- [1] Ehrlich P. *Das Sauerstoffbedürfnis des Organismus. Eine farbenanalytische Studie.* Berlin: Hirschwald; 1885.
- [2] Lewandowsky M. *Zur Lehre von der. Cerebrospinalflüssigkeit.* *Z Klin Med* 1900;40:480–94.
- [3] Goldmann E. *Vitalfärbung am Zentralnervensystem.* *Abhandl Konigpreuss Akad Wiss* 1913;1:1–60.
- [4] Davson H, Spaziani E. The blood–brain barrier and the extracellular space of brain. *J Physiol* 1959;149:135–43.
- [5] Reese T, Karnovsky M. Fine structural localization of a blood–brain barrier to exogenous peroxidase. *J Biol Chem* 1967;34:207–17.
- [6] Pardridge WM. Advances in cell biology of blood–brain barrier transport. *Semin Cell Biol* 1991;2:419–26.
- [7] Pardridge WM. Drug and gene delivery to the brain: the vascular route. *Neuron* 2002;36:555–8.
- [8] Pardridge WM. The blood–brain barrier: bottleneck in brain drug development. *NeuroRx* 2005;2:3–14.
- [9] Staddon JM, Rubin LL. Cell adhesion, cell junctions and the blood–brain barrier. *Curr Opin Neurobiol* 1996;6:622–7.
- [10] Abbott NJ, Rönnbäck L, Hansson E. Astrocyte–endothelial interactions at the blood–brain barrier. *Nat Rev Neurosci* 2006;7:41–53.
- [11] Stewart PA, Tuor UI. Blood–eye barriers in the rat: correlation of ultrastructure with function. *J Comp Neurol* 1994;340:566–76.
- [12] Pardridge WM. Blood–brain barrier drug targeting: the future of brain drug development. *Mol Interv* 2003;3:90–105.
- [13] Kroll RA, Neuwelt EA. Outwitting the blood–brain barrier for therapeutic purposes: osmotic opening and other means. *Neurosurgery* 1998;42:1083–99.
- [14] Lo EH, Singhal AB, Torchilin VP, et al. Drug delivery to damaged brain. *Brain Res Rev* 2001;38:140–8.
- [15] Gulyaev AE, Gelperina SE, Skidan IN, et al. Significant transport of doxorubicin into the brain with polysorbate 80-coated nanoparticles. *Pharm Res* 1999;16:1564–9.
- [16] Singh M. Transferrin as a targeting ligand for liposomes and anticancer drugs. *Curr Pharm Des* 1999;5:443–51.
- [17] Pardridge WM, Kang YS, Buciak JL. Transport of human recombinant brain-derived neurotrophic factor (BDNF) through the rat blood–brain barrier *in vivo* using vector-mediated peptide drug delivery. *Pharm Res* 1994;11:738–46.
- [18] Schwarze SR, Ho A, Vocero-Akbani A, et al. *In vivo* protein transduction: delivery of a biologically active protein into the mouse. *Science* 1999;285:1569–72.
- [19] Pan GY, Liu XD, Liu GQ. Intracarotid infusion of hypertonic mannitol changes permeability of blood–brain barrier to methotrexate in rats. *Acta Pharmacol Sin* 2000;21:613–6.
- [20] Dietz GP, Bahr M. Delivery of bioactive molecules into the cell: the Trojan horse approach. *Mol Cell Neurosci* 2004;27:85–131.
- [21] Shoichet MS, Winn SR. Cell delivery to the central nervous system. *Adv Drug Deliv Rev* 2000;42:81–102.
- [22] Burger FJ, Fuhrman FA. Evidence of injury by heat in mammalian tissues. *Am J Physiol* 1964;206:1057–61.
- [23] Diederich CJ, Hynynen K. Ultrasound technology for hyperthermia. *Ultrasound Med Biol* 1999;25:871–87.
- [24] Chan AH, Fujimoto VY, Moore DE, et al. An image-guided high intensity focused ultrasound device for uterine fibroids treatment. *Med Phys* 2002;29:2611–20.
- [25] Chapelon JY, Ribault M, Vernier F, et al. Treatment of localised prostate cancer with transrectal high intensity focused ultrasound. *Eur J Ultrasound* 1999;9:31–8.
- [26] Hwang JH, Vaezy S, Martin RW, et al. High-intensity focused US: a potential new treatment for GI bleeding. *Gastrointest Endosc* 2003;58:111–5.
- [27] Noble ML, Vaezy S, Keshavarzi A, et al. Spleen hemostasis using high-intensity ultrasound: survival and healing. *J Trauma* 2002;53:1115–20.
- [28] Hynynen K, Jolesz FA. Demonstration of potential noninvasive ultrasound brain therapy through an intact skull. *Ultrasound Med Biol* 1998;24:275–83.
- [29] Pernot M, Aubry JF, Tanter M, et al. High power transcranial beam steering for ultrasonic brain therapy. *Phys Med Biol* 2003;48:2577–89.



- [30] Yin X, Hynynen K. A numerical study of transcranial focused ultrasound beam propagation at low frequency. *Phys Med Biol* 2005;50:1821–36.
- [31] Sokka SD, King R, Hynynen K. MRI-guided gas bubble enhanced ultrasound heating in *in vivo* rabbit thigh. *Phys Med Biol* 2003;48:223–41.
- [32] Shi WT, Forsberg F. Ultrasonic characterization of the nonlinear properties of contrast microbubbles. *Ultrasound Med Biol* 2000;26:93–104.
- [33] Lentacker I, Smedta SCD, Sanders NN. Drug loaded microbubble design for ultrasound triggered delivery. *Soft Matter* 2009;5:2161–70.
- [34] Wu J, Ross JP, Chiu JF. Repairable sonoporation generated by microstreaming. *J Acoust Soc Am* 2002;111:1460–4.
- [35] Liu HL, Wai YY, Chen WS, et al. Hemorrhage detection during focused-ultrasound induced blood–brain-barrier opening by using susceptibility-weighted magnetic resonance imaging. *Ultrasound Med Biol* 2008;34:598–606.
- [36] Hynynen K, McDannold N, Vykhodtseva N, et al. Noninvasive MR imaging-guided focal opening of the blood–brain barrier in rabbits. *Radiology* 2001;154:640–6.
- [37] Yang FY, Lin YS, Kang KH, et al. Reversible blood–brain barrier disruption by repeated transcranial focused ultrasound allows enhanced extravasation. *J Control Release* 2011;150:111–6.
- [38] Xie F, Boska MD, Lof J, et al. Effects of transcranial ultrasound and intravenous microbubbles on blood brain barrier permeability in a large animal model. *Ultrasound Med Biol* 2008;34:2028–34.
- [39] Liu HL, Chen PY, Yang HW, et al. *In vivo* MR quantification of superparamagnetic iron oxide nanoparticle leakage during low-frequency-ultrasound-induced blood–brain barrier opening in swine. *J Magn Reson Imaging* 2011;34:1313–24.
- [40] McDannold N, Arvanitis CD, Vykhodtseva N, et al. Temporary disruption of the blood–brain barrier by use of ultrasound and microbubbles: safety and efficacy evaluation in rhesus macaques. *Cancer Res* 2012;72:3652–63.
- [41] Marquet F, Tung YS, Teichert T, et al. Noninvasive, transient and selective blood–brain barrier opening in non-human primates *in vivo*. *PLoS One* 2011;6:e22598.
- [42] Tung YS, Marquet F, Teichert T, et al. Feasibility of noninvasive cavitation-guided blood–brain barrier opening using focused ultrasound and microbubbles in nonhuman primates. *Appl Phys Lett* 2011;98:163704.
- [43] Sheikov N, McDannold N, Vykhodtseva N, et al. Cellular mechanisms of the blood–brain barrier opening induced by ultrasound in presence of microbubbles. *Ultrasound Med Biol* 2004;30:979–89.
- [44] Hynynen K, McDannold N, Sheikov N, et al. Local and reversible blood–brain barrier disruption by noninvasive focused ultrasound at frequencies suitable for trans-skull sonications. *NeuroImage* 2005;24:12–20.
- [45] Deng J, Huang Q, Wang F, et al. The role of caveolin-1 in blood–brain barrier disruption induced by focused ultrasound combined with microbubbles. *J Mol Neurosci* 2012;46:677–87.
- [46] Xia CY, Zhang Z, Xue YX, et al. Mechanisms of the increase in the permeability of the blood–tumor barrier obtained by combining low-frequency ultrasound irradiation with small-dose bradykinin. *J Neurooncol* 2009;94:41–50.
- [47] Hynynen K, McDannold N, Vykhodtseva N, et al. Focal disruption of the blood-brain barrier due to 260-kHz ultrasound bursts—a method for molecular imaging and targeted drug delivery. *J Neurosurg* 2006;105:445–54.
- [48] Jalali S, Huang Y, Dumont DJ, et al. Focused ultrasound-mediated BBB disruption is associated with an increase in activation of AKT: experimental study in rats. *BMC Neurol* 2010;10:114–24.
- [49] Shang X, Wang P, Liu Y, et al. Mechanism of low-frequency ultrasound in opening blood–tumor barrier by tight junction. *J Mol Neurosci* 2011;43:364–9.
- [50] Raymond SB, Skoch J, Hynynen K, et al. Multi-photon imaging of ultrasound/Optison mediated cerebrovascular effects *in vivo*. *J Cereb Blood Flow Metab* 2007;27:393–403.
- [51] Park J, Fan Z, Kumon RE, et al. Modulation of intracellular  $Ca^{2+}$  concentration in brain microvascular endothelial cells *in vitro* by acoustic cavitation. *Ultrasound Med Biol* 2010;36:1176–87.
- [52] Cho EE, Drazic J, Ganguly M, et al. Two-photon fluorescence microscopy study of cerebrovascular dynamics in ultrasound-induced blood–brain barrier opening. *J Cereb Blood Flow Metab* 2011;31:1852–62.
- [53] McDannold N, Vykhodtseva N, Hynynen K. Targeted disruption of the blood–brain barrier with focused ultrasound: association with cavitation activity. *Phys Med Biol* 2006;51:793–807.
- [54] Tung YS, Vlachos F, Choi JJ, et al. *In vivo* transcranial cavitation threshold detection during ultrasound-induced blood–brain barrier opening in mice. *Phys Med Biol* 2010;55:6141–55.
- [55] Xi G, Keep RF, Hoff JT. Mechanisms of brain injury after intracerebral haemorrhage. *Lancet Neurol* 2006;5:53–63.
- [56] Liu HL, Hua MY, Chen PY, et al. Blood–brain barrier disruption with focused ultrasound enhances delivery of chemotherapeutic drugs for glioblastoma treatment. *Radiology* 2010;255:415–25.
- [57] Qureshi AI, Ling GS, Khan J, et al. Quantitative analysis of injured, necrotic, and apoptotic cells in a new experimental model of intracerebral hemorrhage. *Crit Care Med* 2001;29:152–7.
- [58] Ropper AH. Lateral displacement of the brain and level of consciousness in patients with an acute hemispherical mass. *N Engl J Med* 1986;314:953–8.
- [59] Mayer SA, Lignelli A, Fink ME, et al. Perilesional blood flow and edema formation in acute intracerebral hemorrhage: a SPECT study. *Stroke* 1998;29:1791–8.
- [60] Xi G, Keep RF, Hoff JT. Erythrocytes and delayed brain edema formation following intracerebral hemorrhage in rats. *J Neurosurg* 1998;89:991–6.
- [61] Hua Y, Xi G, Keep RF, et al. Complement activation in the brain after experimental intracerebral hemorrhage. *J Neurosurg* 2000;92:1016–22.
- [62] Nakamura T, Keep R, Hua Y, et al. Deferoxamine-induced attenuation of brain edema and neurological deficits in a rat model of intracerebral hemorrhage. *J Neurosurg* 2004;100:672–8.
- [63] Nakamura T, Xi G, Park JW, et al. Holo-transferrin and thrombin can interact to cause brain damage. *Stroke* 2005;36:348–52.
- [64] Yang FY, Fu WM, Chen WS, et al. Quantitative evaluation of the use of microbubbles with transcranial focused ultrasound on blood–brain-barrier disruption. *Ultrasound Sonochem* 2008;15:636–43.
- [65] Kinoshita M, McDannold N, Jolesz FA, et al. Targeted delivery of antibodies through the blood–brain barrier by MRI-guided focused ultrasound. *Biochem Biophys Res Commun* 2006;340:1085–90.
- [66] Yang FY, Horng SC, Lin YS, et al. Association between contrast-enhanced MR images and blood–brain barrier disruption following transcranial focused ultrasound. *J Magn Reson Imaging* 2010;32:593–9.
- [67] Vlachos F, Tung YS, Konofagou EE. Permeability dependence study of the focused ultrasound-induced blood–brain barrier opening at distinct pressures and microbubble diameters using DCE-MRI. *Magn Reson Med* 2011;66:821–30.

- [68] Sheikov N, McDannold N, Jolesz F, et al. Brain arterioles show more active vesicular transport of blood-borne tracer molecules than capillaries and venules after focused ultrasound-evoked opening of the blood–brain barrier. *Ultrasound Med Biol* 2006;32:1399–409.
- [69] Sheikov N, McDannold N, Sharma S, et al. Effect of focused ultrasound applied with an ultrasound contrast agent on the tight junctional integrity of the brain microvascular endothelium. *Ultrasound Med Biol* 2008;34:1093–104.
- [70] Yang FY, Wang HE, Lin GL, et al. Micro-SPECT/CT-based pharmacokinetic analysis of <sup>99m</sup>Tc-diethylenetriaminepentaacetic acid in rats with blood–brain barrier disruption induced by focused ultrasound. *J Nucl Med* 2011;52:478–84.
- [71] Liu HL, Hsu PH, Chu PN, et al. Magnetic resonance imaging enhanced by superparamagnetic iron oxide particles: Usefulness for distinguishing between focused ultrasound-induced blood–brain barrier disruption and brain hemorrhage. *J Magn Reson Imaging* 2009;29:31–8.
- [72] Howles GP, Bing KF, Qi Y, et al. Contrast-enhanced *in vivo* magnetic resonance microscopy of the mouse brain enabled by noninvasive opening of the blood–brain barrier with ultrasound. *Magn Reson Med* 2010;64:995–1004.
- [73] Wang PH, Liu HL, Hsu PH, et al. Gold-nanorod contrast-enhanced photoacoustic micro-imaging of focused-ultrasound induced blood–brain-barrier opening in a rat model. *J Biomed Opt* 2012;17:061222.
- [74] Kinoshita M, McDannold N, Jolesz FA, et al. Noninvasive localized delivery of Herceptin to the mouse brain by MRI-guided focused ultrasound-induced blood–brain barrier disruption. *Proc Natl Acad Sci U S A* 2006;103:11719–23.
- [75] Treat LH, McDannold N, Vykhodtseva N, et al. Targeted delivery of doxorubicin to the rat brain at therapeutic levels using MRI-guided focused ultrasound. *Int J Cancer* 2007;121:901–7.
- [76] Wu F, Wang ZB, Chen WZ, et al. Extracorporeal high intensity focused ultrasound ablation in the treatment of patients with large hepatocellular carcinoma. *Ann Surg Oncol* 2004;11:1061–9.
- [77] Treat L, Zhang Y, McDannold N, et al. MRI-guided focused ultrasound-enhanced chemotherapy of 9 l rat gliosarcoma: survival study. *Proceeding of the International Society for Magnetic Resonance in Medicine*, vol. 16; 2008.
- [78] Wei KC, Chu PC, Wang HY, et al. Focused ultrasound-induced blood-brain barrier opening to enhance temozolomide delivery for glioblastoma treatment: a preclinical study. *PLoS One* 2013;8:e58995.
- [79] Yang FY, Chen YW, Chou FI, et al. Boron neutron capture therapy for glioblastoma multiforme: enhanced drug delivery and antitumor effect following blood-brain barrier disruption induced by focused ultrasound. *Future Oncol* 2012;8:1361–9.
- [80] Alkins RD, Brodersen PM, Sodhi RN, et al. Enhancing drug delivery for boron neutron capture therapy of brain tumors with focused ultrasound. *Neuro Oncol* 2013;15:1225–35.
- [81] Jordão JF, Ayala-Grosso CA, Markham K, et al. Antibodies targeted to the brain with image-guided focused ultrasound reduces amyloid-beta plaque load in the TgCRND8 mouse model of Alzheimer's disease. *PLoS One* 2010;5:e10549.
- [82] Raymond SB, Treat LH, Dewey JD, et al. Ultrasound enhanced delivery of molecular imaging and therapeutic agents in Alzheimer's disease mouse models. *PLoS One* 2008;3:e2175.
- [83] Burgess A, Ayala-Grosso CA, Ganguly M, et al. Targeted delivery of neural stem cells to the brain using MRI-guided focused ultrasound to disrupt the blood–brain barrier. *PLoS One* 2011;6:e27877.
- [84] Burgess A, Huang Y, Querbes W, et al. Focused ultrasound for targeted delivery of siRNA and efficient knockdown of Htt expression. *J Control Release* 2012;163:125–9.
- [85] Burgess A, Huang Y, Querbes W, et al. Non-invasive delivery of small interfering ribonucleic acid for reduction of Huntingtin expression in the brain is achieved using focused ultrasound to disrupt the blood–brain barrier. *J Acoust Soc Am* 2013;133:3408.
- [86] Huang Q, Deng J, Wang F, et al. Targeted gene delivery to the mouse brain by MRI-guided focused ultrasound-induced blood–brain barrier disruption. *Exp Neurol* 2012;233:350–6.
- [87] Hsu PH, Wei KC, Huang CY, et al. Noninvasive and targeted gene delivery into the brain using microbubble-facilitated focused ultrasound. *PLoS One* 2013;8:e57682.
- [88] Jemal A, Siegel R, Ward E, et al. *Cancer statistics, 2006*. *CA Cancer J Clin* 2006;56:106–30.
- [89] Behin A, Hoang-Xuan K, Carpentier AF, et al. Primary brain tumours in adults. *Lancet* 2003;361:323–31.
- [90] Ewing JR, Brown SL, Lu M, et al. Model selection in magnetic resonance imaging measurements of vascular permeability: gadomer in a 9L model of rat cerebral tumor. *J Cereb Blood Flow Metab* 2006;26:310–20.
- [91] Neuwelt EA, Frenkel EP, D'Agostino AN. Growth of human lung tumor in the brain of the nude rat as a model to evaluate antitumor agent delivery across the blood–brain barrier. *Cancer Res* 1985;45:2827–33.
- [92] Groothuis DR, Fischer JM, Lapin G, et al. Permeability of different experimental brain tumor models to horseradish peroxidase. *J Neuropathol Exp Neurol* 1985;41:164–85.
- [93] Park EJ, Zhang YZ, Vykhodtseva N, et al. Ultrasound-mediated blood–brain/blood–tumor barrier disruption improves outcomes with trastuzumab in a breast cancer brain metastasis model. *J Control Release* 2012;163:277–84.
- [94] Fan CH, Ting CY, Lin HJ, et al. SPIO-conjugated, doxorubicin-loaded microbubbles for concurrent MRI and focused-ultrasound enhanced brain-tumor drug delivery. *Biomaterials* 2013;34:3706–15.
- [95] Liu HL, Hua MY, Yang HW, et al. Magnetic resonance monitoring of focused ultrasound magnetic nanoparticle targeting delivery of therapeutic agents to the brain. *Proc Natl Acad Sci U S A* 2010;107:15205–10.
- [96] Liu HL, Hsieh HY, Lu LA, et al. Low-pressure pulsed focused ultrasound with microbubbles promotes an anticancer immunological response. *J Transl Med* 2012;10:221–35.
- [97] Beal MF. Parkinson's disease: a model dilemma. *Nature* 2010;466:8–10.
- [98] Strauss I, Kalia SK, Lozano AM. Where are we with surgical therapies for Parkinson's disease? *Parkinsonism Relat Disord* 2014;20:S187–91.
- [99] Wang X, Guo S, Lu S, et al. Ultrasound-induced release of GDNF from lipid coated microbubbles injected into striatum reduces hypoxic-ischemic injury in neonatal rats. *Brain Res Bull* 2012;88:495–500.
- [100] Wang X, Cui G, Yang X, et al. Intracerebral administration of ultrasound-induced dissolution of lipid-coated GDNF microbubbles provides neuroprotection in a rat model of Parkinson's disease. *Brain Res Bull* 2014;103:60–5.
- [101] Waldemar G, Dubois B, Emre M, et al. Recommendations for the diagnosis and management of Alzheimer's disease and other disorders associated with dementia: EFNS guideline. *Eur J Neurol* 2007;14:e1–26.
- [102] Tabert MH, Liu X, Doty RL, et al. A 10-item smell identification scale related to risk for Alzheimer's disease. *Ann Neurol* 2005;58:155–60.
- [103] Ingelsson M, Hyman B. Disordered proteins in dementia. *Ann Med* 2002;34:259–71.
- [104] Thakker DR, Weatherspoon MR, Harrison J, et al. Intracerebroventricular amyloid-beta antibodies reduce cerebral amyloid angiopathy and associated micro-hemorrhages in aged Tg2576 mice. *Proc Natl Acad Sci U S A* 2009;106:4501–6.

- [105] Kotilinek LA, Bacskai B, Westerman M, et al. Reversible memory loss in a mouse transgenic model of Alzheimer's disease. *J Neurosci* 2002;22:6331–5.
- [106] Wilcock DM, Colton CA. Anti-amyloid-beta immunotherapy in Alzheimer's disease: relevance of transgenic mouse studies to clinical trials. *J Alzheimers Dis* 2008;15:555–69.
- [107] Banks WA, Terrell B, Farr SA, et al. Passage of amyloid beta protein antibody across the blood–brain barrier in a mouse model of Alzheimer's disease. *Peptides* 2002;23:2223–6.
- [108] Wilcock DM, DiCarlo G, Henderson D, et al. Intracranially administered anti-Abeta antibodies reduce beta-amyloid deposition by mechanisms both independent of and associated with microglial activation. *J Neurosci* 2003;23:3745–51.
- [109] Jordão JF, Thévenot E, Markham-Coultes K, et al. Amyloid- $\beta$  plaque reduction, endogenous antibody delivery and glial activation by brain-targeted, transcranial focused ultrasound. *Exp Neurol* 2013;248:16–29.
- [110] Burgess A, Dubey S, Yeung S, et al. Alzheimer disease in a mouse model: MR imaging-guided focused ultrasound targeted to the hippocampus opens the blood–brain barrier and improves pathologic abnormalities and behavior. *Radiology* 2014;273:736–45.
- [111] Burgess A, Nhan T, Moffatt C, et al. Analysis of focused ultrasound-induced blood-brain barrier permeability in a mouse model of Alzheimer's disease using two-photon microscopy. *J Control Release* 2014;192c:243–8.
- [112] Zuccato C, Valenza M, Cattaneo E. Molecular mechanisms and potential therapeutical targets in Huntington's disease. *Physiol Rev* 2010;90:905–81.
- [113] Shen V, Clarence-Smith K, Hunter C, et al. Safety and efficacy of tetrabenazine and use of concomitant medications during long-term, open-label treatment of chorea associated with Huntington's and other diseases. *Tremor Other Hyperkinet Mov (N Y)* 2013;3.
- [114] Robertson MM. Tourette syndrome, associated conditions and the complexities of treatment. *Brain* 2000;123:425–62.
- [115] DiFiglia M, Sena-Esteves M, Chase K, et al. Therapeutic silencing of mutant huntingtin with siRNA attenuates striatal and cortical neuropathology and behavioral deficits. *Proc Natl Acad Sci U S A* 2007;104:17204–9.
- [116] O'Reilly MA, Huang Y, Hynynen K. The impact of standing wave effects on transcranial focused ultrasound disruption of the blood–brain barrier in a rat model. *Phys Med Biol* 2010;55:5251–67.
- [117] White PJ, Clement GT, Hynynen K. Longitudinal and shear mode ultrasound propagation in human skull bone. *Ultrasound Med Biol* 2006;32:1085–96.
- [118] Clement GT, Sun J, Giesecke T, et al. A hemisphere array for non-invasive ultrasound brain therapy and surgery. *Phys Med Biol* 2000;45:3707–19.
- [119] Vlachos F, Tung YS, Konofagou EE. Permeability assessment of the focused ultrasound-induced blood–brain barrier opening using dynamic contrast-enhanced MRI. *Phys Med Biol* 2010;55:5451–66.
- [120] Liu HL, Wai YY, Hsu PH, et al. *In vivo* assessment of macrophage CNS infiltration during disruption of the blood–brain barrier with focused ultrasound: a magnetic resonance imaging study. *J Cereb Blood Flow Metab* 2010;30:177–86.
- [121] Goertz DE, Wright C, Hynynen K. Contrast agent kinetics in the rabbit brain during exposure to therapeutic ultrasound. *Ultrasound Med Biol* 2010;36:916–24.
- [122] Fan CH, Lin WH, Ting CY, et al. Contrast-enhanced ultrasound imaging for the detection of focused ultrasound-induced blood–brain barrier opening. *Theranostics* 2014;4:1014–25.
- [123] Fan CH, Liu HL, Ting CY, et al. Submicron-bubble-enhanced focused ultrasound for blood–brain barrier disruption and improved CNS drug delivery. *PLoS One* 2014;9:e96327.
- [124] O'Reilly MA, Hynynen K. Blood–brain barrier: real-time feedback-controlled focused ultrasound disruption by using an acoustic emissions-based controller. *Radiology* 2012;263:96–106.
- [125] Yang FY, Chen CC, Kao YH, et al. Evaluation of dose distribution of molecular delivery after blood–brain barrier disruption by focused ultrasound with treatment planning. *Ultrasound Med Biol* 2013;39:620–7.
- [126] Park J, Zhang Y, Vykhodtseva N, et al. The kinetics of blood brain barrier permeability and targeted doxorubicin delivery into brain induced by focused ultrasound. *J Control Release* 2012;162:134–42.
- [127] Chai WY, Chu PC, Tsai MY, et al. Magnetic-resonance imaging for kinetic analysis of permeability changes during focused ultrasound-induced blood–brain barrier opening and brain drug delivery. *J Control Release* 2014;192:1–9.
- [128] Fan CH, Ting CY, Liu HL, et al. Antiangiogenic-targeting drug-loaded microbubbles combined with focused ultrasound for glioma treatment. *Biomaterials* 2013;34:2142–55.
- [129] Ting CY, Fan CH, Liu HL, et al. Concurrent blood-brain barrier opening and local drug delivery using drug-carrying microbubbles and focused ultrasound for brain glioma treatment. *Biomaterials* 2012;33:704–12.